Available online at www.sciencedirect.com
ScienceDirect
Trans. Nonferrous Met. Soc. China 23(2013) 3598−3603
Transactions of Nonferrous Metals Society of China
www.tnmsc.cn

Microstructure and mechanical properties of $Mg_{94}Zn_2Y_4$ extruded alloy with long-period stacking ordered structure

Huan LIU [1], Feng XUE[1,2], Jing BAI[1,2], Jian ZHOU[1,2], Yang-shan SUN[1,2]

1. School of Materials Science and Engineering, Southeast University, Nanjing 211189,China;
2. Jiangsu Key Laboratory for Advanced Metallic Materials, Southeast University, Nanjing 211189,China

Received 22 August 2012; accepted 22 October 2012

Abstract: The microstructure and mechanical properties of $Mg_{94}Zn_2Y_4$ extruded alloy containing long-period stacking ordered structures were systematically investigated by SEM and TEM analyses. The results show that the 18R-LPSO structure and α-Mg phase are observed in cast $Mg_{94}Zn_2Y_4$ alloy. After extrusion, the LPSO structures are delaminated and Mg-slices with width of 50−200 nm are generated. By ageing at 498 K for 36 h, the ageing peak is attained and β' phase is precipitated. Due to this novel precipitation, the microhardness of α-Mg matrix increases apparently from HV108.9 to HV129.7. While the microhardness for LPSO structure is stabilized at about HV145. TEM observations and SAED patterns indicate that the β' phase has unique orientation relationships between α-Mg and LPSO structures, the direction in the close-packed planes of β' precipitates perpendicular to that of α-Mg and LPSO structures. The ultimate tensile strength for the peak-aged alloy achieves 410.7 MPa and the significant strength originates from the coexistence of β' precipitates and 18R-LPSO structures.

Key words: $Mg_{94}Zn_2Y_4$ alloy; long-period stacking ordered structure; precipitation; ageing; tensile property

1 Introduction

Magnesium alloys with rare element (RE) metals are currently of great interest for applications in aerospace and automotive industries due to their extraordinarily low density, high specific strength and easy-recycling ability. However, the relatively low strength and poor heat resistant properties strongly restrict their further spread for powertrain applications [1,2]. Therefore, great efforts have been expended to improve the mechanical properties of Mg−RE alloys.

Recently, KAWAMURA et al [3] developed a $Mg_{97}Zn_1Y_2$ alloy by warm extrusion of rapidly solidified powders at 573 K which exhibited a high yield strength of 610 MPa with 5% elongation at room temperature. The high strength of this alloy derives from the ultrafine α-Mg grains and the appearance of a novel long-period stacking ordered (LPSO) structure, which was identified to be a chemical and stacking ordered structure with 6 atomic planes in a single period. Afterwards, various LPSO phases of 10H, 14H, 18R and 24R types have been observed in other kinds of Mg−RE−Zn ternary systems, and the mechanical properties of these alloys have been investigated [4−6]. The LPSO-containing alloys exhibit superior performance after conventional deformation processes like rolling, extruding, etc [7,8]. Usually, the extruded $Mg_{97}Zn_1Y_2$ alloy displays a high tensile strength of approximately 350 MPa at RT with appreciable ductility [9], which is still not high enough for use in components of aircrafts and automobiles.

Since the RE elements usually have a large solid solubility in Mg−RE alloys and the solubility decreases drastically as temperature drops, precipitation strengthening is another attractive way to improve the mechanical properties of these alloys [10]. Consequently, the combination of LPSO phases and precipitates in Mg−RE−Zn alloys might greatly enhance the properties of the alloys. In addition, although the LPSO/precipitate systems were observed in Mg−Gd−Y−Zn−Zr [10] and Mg−Zn−Y−Nd alloys [11], the precipitates have not been reported in LPSO-containing Mg−Zn−Y ternary alloys by now. Therefore, the objective of the present study is to explore the formation of RE-containing

Foundation item: Project (BK2010392) supported by the Natural Science Foundation of Jiangsu Province of China; Project (3212000502) supported by the Innovation Foundation of Southeast University, China
Corresponding author: Feng XUE; Tel: +86-25-52090689; E-mail: xuefeng@seu.edu.cn
DOI: 10.1016/S1003-6326(13)62906-4

precipitates together with LPSO phases existing in Mg−Zn−Y ternary systems. In this work, the phase compositions, ageing hardening behavior, microstructure and tensile properties of the as-extruded and peak-aged $Mg_{94}Zn_2Y_4$ alloy are investigated, which is expected to provide useful information for optimizing the mechanical properties via microstructures of new magnesium alloys.

2 Experimental

An alloy ingot of $Mg_{94}Zn_2Y_4$ (mole fraction, %) was prepared from pure Mg, Zn and Y metals by melting in an electric resistance furnace with a mild steel crucible under the protective gas of mixed CO_2 and SF_6. After being remelted at 1023 K for 0.5 h, the melt was poured into a water-cooling copper mold with inside diameter of 60 mm. Homogenized at 773 K for 12 h, the alloy ingot was then extruded at 703 K with an extrusion ratio of 9:1 and quenched in air. Rods with diameter of 20 mm were then aged at 498 K for a total time of 80 h in a furnace. Microhardness of the alloy was measured by FM700 microhardness tester at a load of 0.98 N with loading time of 10 s. The tensile test was carried out on an electronic universal testing machine with the tensile axis parallel to the extrusion direction at a cross-head speed of 2 mm/min at room temperature. The microstructures were examined with an optical microscope (OM; Olympus BHM), a scanning electron microscope (SEM; FEI Sirion 200) equipped with an X-ray energy dispersive spectrometer (EDS) and a transmission electron microscope (TEM; JOEL−2000EX). Samples for OM and SEM observations were mechanically polished and then etched with 4 mL nitric acid and 96 mL ethanol. To obtain the TEM image, specimens were thinned by twin-jet electro polishing in a solution of 5% perchloric acid and 95% ethanol.

3 Results and discussion

3.1 Microstructures of as-cast and as-extruded $Mg_{94}Zn_2Y_4$ alloy

Figure 1(a) shows the SEM backscatter electron image (BEI) of the cast $Mg_{94}Zn_2Y_4$ alloy. Two phases are well observed, the α-Mg matrix and a secondary phase with lamellar morphology distributed in the interdendritic region. The EDS results reveal that the compositions for the black and white regions are Mg−2.92%Y−0.58%Zn and Mg−7.33%Y−4.96%Zn (mole fraction), respectively. The composition of the secondary phase is consistent with *X*-phase, which was reported to be a long-period stacking ordered structure by LUO et al [12]. The TEM selected area electron diffraction (SAED) pattern of the intermetallic phase is shown in Fig. 1(b). It is clear that five extra diffracting spots occur at the $1/6(0002)_\alpha$, $2/6(0002)_\alpha$, $3/6(0002)_\alpha$, $4/6(0002)_\alpha$, and $5/6(0002)_\alpha$ positions, which is the evidence commonly used to prove the existence of the 18R structure [13]. Besides, five sets of weak streaks appear along the $(0001)_\alpha$ direction and through

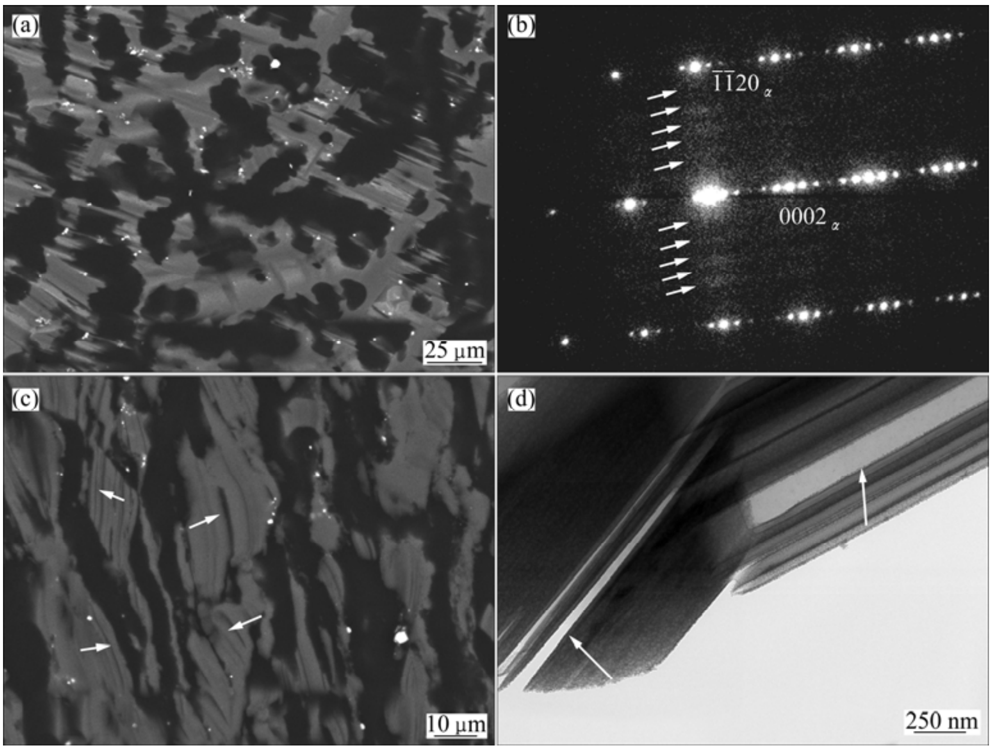

Fig. 1 BEI (a) and SAED pattern of as-cast $Mg_{94}Zn_2Y_4$ alloy (b), and BEI (c) of and TEM image (d) of as-extruded alloy

$\pm 1/6\{\bar{1}120\}_\alpha$, $\pm 2/6\{\bar{1}120\}_\alpha$, $\pm 3/6\{\bar{1}120\}_\alpha$, $\pm 4/6\{\bar{1}120\}_\alpha$ and $\pm 5/6\{1120\}_\alpha$ positions. Moreover, the streaks through the $\pm 2/6\{\bar{1}120\}_\alpha$, $\pm 3/6\{\bar{1}120\}_\alpha$ and $\pm 4/6\{\bar{1}120\}_\alpha$ positions show comparatively stronger intensities than those through the $\pm 1/6\{1120\}_\alpha$ and $\pm 1/6\{\bar{1}120\}_\alpha$ positions. The appearance of these streaks confirm that the secondary phase is 18R LPSO structure [13]. Also, from the SAED pattern it can be seen that the orientation relationships between α-Mg matrix and LPSO phase are $(001)_{2H\text{-}Mg}//(0018)_{18R\text{-}LPSO}$ and $[001]_{2H\text{-}Mg}//[001]_{18R\text{-}LPSO}$.

Figure 1(c) shows the BEI of the $Mg_{94}Zn_2Y_4$ alloy in as-extruded condition. During extrusion, the LPSO network is broken and the LPSO phase is aligned along the direction of extrusion. Parts of the LPSO structures are deformed and fragment into smaller pieces. As for coarse LPSO, kinking bands are formed and delamination of LPSO phases also appears in abundant regions, as indicated by arrows in Fig. 1(c). A bright field TEM image of the extruded LPSO phase is shown in Fig. 1(d). Gaps with sizes of 50−200 nm are observed between delaminated LPSO structures, as marked by arrows. Interfaces between the delaminated LPSO phase and Mg matrix in the gaps are distinct and smooth, while no cracks are observed, indicating a good connection and excellent ductility of LPSO phase.

3.2 Precipitation behavior

Figure 2 displays the precipitation hardening curve of the as-extruded specimens aged at 498 K for 80 h. The alloy exhibits a remarkable age hardening response. The hardness of the as-extruded alloy is HV117, which

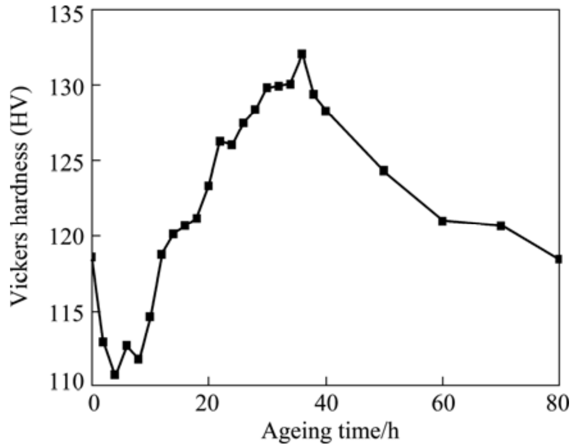

Fig. 2 Hardness variation of alloy aged at 498 K as function of ageing time

decreases obviously in the first 10 h of ageing, and then increases significantly. Peak hardness of HV132 is obtained at 36 h. After that point the hardness decreases gradually with ageing time.

Figure 3(a) shows the SEM (BEI) image of the $Mg_{94}Zn_2Y_4$ alloy aged at 498 K for 36 h. Compared with the as-extruded alloy, there is no obvious difference for the morphology of LPSO structures. Figure 3(b) shows the bright field (BF) TEM image of the α-Mg matrix. It can be seen that numerous fine particles precipitate in the matrix. The SAED pattern of the matrix is shown in Fig. 3(c). Three extra diffraction spots locate at $1/4(01\bar{1}0)_\alpha$, $2/4(01\bar{1}0)_\alpha$ and $3/4(01\bar{1}0)_\alpha$ positions, indicating that the precipitate is β' phase. Its structure is

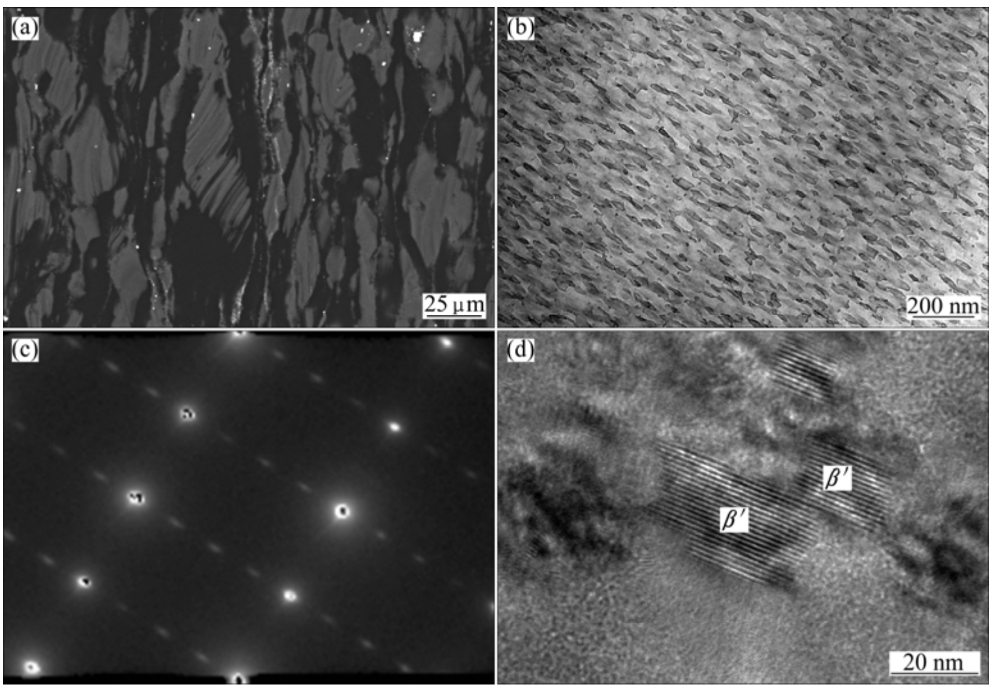

Fig. 3 Microstructures of peak-aged $Mg_{94}Zn_2Y_4$ alloy: (a) SEM image; (b) BF TEM image; (c) SAED pattern; (d) HR TEM image

identified as base-centered orthorhombic (BCO) structure with lattice parameters $a=2\times a_{\alpha\text{-Mg}}=0.640$ nm, $b=8\times d(01\bar{1}0)_{\alpha\text{-Mg}}=2.223$ nm, $c=c_{\alpha\text{-Mg}}=0.521$ nm [14]. Also, it can be inferred that the orientation relationships between the β' phases and α-Mg are $(001)_{\beta'}//(0001)_{\alpha\text{-Mg}}$ and $[100]_{\beta'}//[2\bar{1}\bar{1}0]_{\alpha\text{-Mg}}$. High resolution (HR) TEM image of the β' precipitates is shown in Fig. 3(d). It is apparent that the average size of β' precipitates is about 20 nm and it has coherent interfaces with α-Mg matrix.

3.3 Mechanical properties

Tensile tests were performed along the extrusion direction for the $Mg_{94}Zn_2Y_4$ alloy and its peak-aged alloy at room temperature. The results are shown in Table 1. Strength for the as-cast alloy is pretty poor, only 130.0 MPa. After extrusion the alloy is strengthened by work hardening and deformed LPSO phase that acts as short-fiber reinforcement. During ageing, β' phases precipitate in the matrix, which further improves the tensile strength. However, the ductility of the alloy needs further enhancement since at all stages the $Mg_{94}Zn_2Y_4$ alloy exhibits poor elongation. Table 2 shows Vickers hardness of the matrix and LPSO phase at different stages. Hardness for the LPSO structures is stable at all three stages and is higher than the matrix, indicating that LPSO phase is a kind of hardening phase. As for the matrix, the hardness is HV 80.8 at as-cast stage and increases to HV108.9 after deformation. The increase originates from work hardening, recrystallization around the LPSO phases and solution strengthening since the extrusion temperature is relatively high which accelerates the diffusion of Y and Zn atoms from the secondary phases to the matrix. After ageing, the increase of hardness for the matrix is mainly owing to

Table 1 Tensile properties of $Mg_{94}Zn_2Y_4$ alloy at different stages

Alloy stage	Yield strength/MPa	Ultimate tensile strength/MPa	Elongation/%
As-cast	96.5	130.0	2.9
As-extruded	246.4	389.6	2.8
Peak-aged	272.3	410.7	2.8

Table 2 Vickers hardness of matrix and LPSO phase at different stages

Alloy stage	Hardness (HV)	
	Matrix	LPSO
As-cast	80.8	143.8
As-extruded	108.9	145.4
Peak-aged	129.7	147.1

the novel precipitates.

It has been reported that the LPSO phase in as-extruded alloys could enhance the mechanical properties of the alloys significantly and the strengthening mechanism was studied elsewhere [15]. Commonly, deformation twin and basal slip are the two positive deformation modes for magnesium alloys at room temperature [16,17]. MATSUDA et al [17] reported that the LPSO phases are effective to stop the growth of $\{10\bar{1}2\}$ deformation twins for $Mg_{97}Zn_1Y_2$ LPSO/Mg alloy. The twins can be deflected or arrested in regions with highly dense LPSO phases. Therefore, the twins are barely observed in the $Mg_{97}Zn_2Y_4$ alloy since the size and quantity of LPSO structures are much greater than those of $Mg_{97}Zn_1Y_2$ alloy. After ageing process, the β' phases precipitate and the close-packed planes of this precipitate are perpendicular to the basal planes of α-Mg matrix. Thus, the movement of dislocations on the basal planes can also be greatly hindered. Since the barrier for the two main deformation modes to activate is promoted, the strength of the alloy is enhanced.

Usually the α-Mg matrix is the weakness of these LPSO-containing alloys, especially the α-Mg slices embedded between LPSO phases [18]. As can be seen in Fig. 1(d), the LPSO phases delaminate elsewhere after extrusion and a plenty of Mg slices with nanoscale in width appear. It is no doubt that the movements of dislocations in the Mg nano-slices are severely restricted. Therefore, once the number of dislocations or stress concentration caused by kinking exceed the capability of the Mg slices to accommodate, microcracks nucleate and propagate from the Mg nano-slices, consequently impiring the alloy. Figure 4(a) shows the bright field image of a Mg-slice embedded in delaminated LPSO phases, where the width of the slice is approximately 50 nm, which is consistent with Fig. 1(d). As shown in Fig. 4(b), three series of patterns appear in the SAED pattern of the slice, representing for the existence of α-Mg, LPSO phase and β' precipitate, respectively. Since the coherent precipitate also exists in the Mg nano-slices, the capability for the slices to accommodate the number and movements of dislocations could be enhanced significantly, resulting in the increase of strength. Besides, it can be seen from the SAED patterns that the diffraction spot lines for β' precipitates are perpendicular to lines for α-Mg and LPSO phases, suggesting the packing direction for β' precipitate in the close-packed planes is perpendicular to that for both α-Mg or LPSO phases. The unique orientation relationships between LPSO phases and β' precipitates might contribute to the increase of strength, and the mechanism should be investigated further.

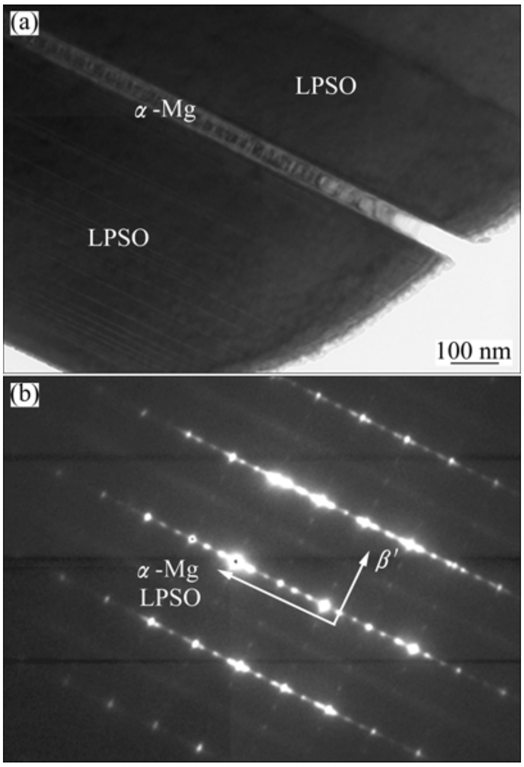

Fig. 4 Bright field image (a) and SAED pattern (b) of α-Mg slice between delaminated LPSO structures

4 Conclusions

1) The microstructure of as-extruded $Mg_{97}Zn_2Y_4$ alloy consists of α-Mg and delaminated 18R-LPSO phase. When aged at 498 K for 36 h, the ageing peak is attained and β' phases are precipitated.

2) After ageing process, the microhardness for the α-Mg matrix and LPSO phases are increased to HV129.7 and HV147.1, respectively. The ultimate tensile strength of the peak-aged alloy achieves 410.7 MPa.

3) The coexistence of β' precipitates and LPSO phases contributes to the strength of the alloy. The α-Mg slices embedded in the delaminated LPSO structures which was used to be the origin of microcracks can be strengthened by β' precipitates.

References

[1] HONMA T, OHKUBO T, KAMADO S, HONO K. Effect of Zn additions on the age-hardening of Mg−2.0Gd−1.2Y−0.2Zr alloys [J]. Acta Mater, 2007, 55(12): 4137−4150.

[2] LIU K, ZHANG J H, TANG D X, ROKHLIN L L, ELKIN F M, MENG J. Precipitates formed in a Mg−7Y−4Gd−0.5Zn−0.4Zr alloy during isothermal ageing at 250 °C [J]. Mater Chem Phys, 2009, 117(1): 107−112.

[3] KAWAMURA Y, HAYASHI K, INOUE A, MASUMOTO T. Rapidly solidified powder metallurgy Mg97Zn1Y2 alloys with excellent tensile yield strength above 600 MPa [J]. Mater Trans, 2001, 42(7): 1172−1176.

[4] MATSUDA M, II S, KAWAMURA Y, IKUHARA Y, NISHIDA M. Variation of long-period stacking order structures in rapidly solidified $Mg_{97}Zn_1Y_2$ alloy [J]. Mater Sci Eng A, 2005, 393(1−2): 269−274.

[5] ITOI T, SEIMIYA T, KAWAMURA Y, HIROHASHI. Long period stacking structures observed in $Mg_{97}Zn_1Y_2$ alloy [J]. Scripta Mater, 2004, 51(2): 107−111.

[6] YAMASAKI M, ANAN T, YOSHIMOTO S, KAWAMURA Y. Mechanical properties of warm-extruded Mg−Zn−Gd alloy with coherent 14H long periodic stacking ordered structure precipitate [J]. Scripta Mater, 2005, 53(7): 799−803.

[7] LI R G, FANG D Q, AN J, LU Y, GAO Z Y, LIU Y B. Comparative studies on the microstructure evolution and fracture behavior between hot-rolled and as-cast $Mg_{96}ZnY_3$ alloys [J]. Mater Charact, 2009, 60(6): 470−475.

[8] HAGIHARA K, KINOSHITA A, SUGINO Y, YAMASAKI M, KAWAMURA Y, YASUDA H Y, UMAKOSHI Y. Plastic deformation behavior of Mg97Zn1Y2 extruded alloy [J]. Transactions of Nonferrous Metals Society of China, 2010, 20(7): 1259−1268.

[9] KAWAMURA Y, KASAHARA T, IZUMI S, YAMASAKI M. Elevated temperature $Mg_{97}Y_2Cu_1$ alloy with long period ordered structure [J]. Scripta Mater, 2006, 55(5): 453−456.

[10] ZHENG L, LIU C M, WAN Y C, YANG P W, SHU X. Microstructures and mechanical properties of Mg−10Gd−6Y−2Zn−0.6Zr(wt.%) alloy [J]. J Alloys Compd, 2011, 509(35): 8832−8839.

[11] LEE J B, SATO K, KONNO T J, HIRAGA K. Complex precipitates with long periodic stacking (LPS) phase and precipitation behaviors in the $Mg_{97}Zn_1Y_{1.5}Nd_{0.5}$ alloy by age-annealing [J]. Intermetallics, 2011, 19(8): 1096−1101.

[12] LUO Z P, ZHANG S Q, TANG Y L, ZHAO D S. Microstructures of Mg−Zn−Zr−RE alloys with high RE and low Zn contents [J]. J Alloys Compd, 1994, 209(1−2): 275−278.

[13] ZHU Y M, MORTON A J, NIE J F. The 18R and 14H long-period stacking ordered structures in Mg−Y−Zn alloys [J]. Acta Mater, 2010, 58(8): 2936−2947.

[14] YIN D D, WANG Q D, GAO Y, CHEN C J, ZHENG J. Effects of heat treatments on microstructure and mechanical properties of Mg−11Y−5Gd−2Zn−0.5Zr [J]. J Alloys Compd, 2011, 509(5): 1696−1704.

[15] HAGIHARA K, KINOSHITA A, SUGINO Y, YAMASAKI M, KAWAMURA Y, YASUDA H Y, UMAKOSHI Y. Effect of long-period stacking ordered phase on mechanical properties of Mg97Zn1Y2 extruded alloy [J]. Acta Mater, 2010, 58(19): 6282−6293.

[16] HAGIHARA K, KINOSHITA A, SUGINO Y, YAMASAKI M, KAWAMURA Y, YASUDA H Y, UMAKOSHI Y. Plastic deformation behavior of Mg89Zn4Y7 extruded alloy composed of long-period stacking ordered phase [J]. Intermetallics, 2010, 18(5): 1079−1085.

[17] MATSUDA M, II S, KAWAMURA Y, IKUHARA Y, NISHIDA M. Interaction between long period stacking order phase and deformation twin in rapidly solidified $Mg_{97}Zn_1Y_2$ alloy [J]. Mater Sci Eng A, 2004, 386(1−2): 447−452.

[18] SHAO X H, YANG Z Q, MA X L. Strengthening and toughening mechanisms in Mg−Zn−Y alloy with a long period stacking ordered structure [J]. Acta Mater, 2010, 58(14): 4760−4771.

含长周期堆垛有序结构 $Mg_{94}Zn_2Y_4$ 挤压态合金的显微组织与力学性能

刘 欢[1]，薛 烽[1,2]，白 晶[1,2]，周 健[1,2]，孙扬善[1,2]

1. 东南大学 材料科学与工程学院，南京 211189；
2. 东南大学 江苏省先进金属材料高技术研究重点实验室，南京 211189

摘 要：采用 SEM 和 TEM 等分析方法研究包含长周期堆垛有序结构的挤压态 $Mg_{94}Zn_2Y_4$ 合金的显微组织和力学性能。结果表明：铸态 $Mg_{94}Zn_2Y_4$ 合金由 18R-LPSO 和 α-Mg 两相组成。挤压后，长周期相分层，并形成宽度为 50~200 nm 的 α-Mg 薄片。合金经 498 K 时效处理 36 h 后达到时效峰值，在其组织中析出 β'相，该析出相的出现显著提高了 α-Mg 基体的显微硬度，从 HV108.9 增加到 HV129.7；而 LPSO 结构的显微硬度稳定在 HV145 左右。TEM 分析及其电子衍射花样表明，β'相与 α-Mg 和 LPSO 结构具有独特的位相关系，其原子最密排面的堆垛方向垂直于 α-Mg 和 LPSO 相最密排面的堆垛方向。由于 β'相和 18R-LPSO 相的共同存在，处于时效峰值态的 $Mg_{94}Zn_2Y_4$ 合金的抗拉强度达到 410.7 MPa。

关键词：$Mg_{94}Zn_2Y_4$ 合金；长周期堆垛有序结构；沉淀；时效；拉伸性能

(Edited by Xiang-qun LI)